

Photon statistics without counting photons

Andrea R. Rossi,^{*} Stefano Olivares,[†] and Matteo G. A. Paris[‡]
Dipartimento di Fisica dell'Università degli Studi di Milano, Italia

(Dated: August 29, 2018)

We show how to obtain the photon distribution of a single-mode field using only avalanche photodetectors. The method is based on measuring the field at different quantum efficiencies and then inferring the photon distribution by maximum-likelihood estimation. The convergence of the method and its robustness against fluctuations are illustrated by means of numerically simulated experiments.

I. INTRODUCTION

Optical signals and nonclassical states of light have been the subject of constant attention over the last three decades. The photon distribution, besides fundamental interest, plays a major role in quantum communication schemes based on light beams, and this stimulated many experiments on the statistical properties of radiation [1]. More recently, the rapid development of quantum information processing once again posed the issue of effective methods to investigate photon statistics [2, 3]. Photon distribution is usually obtained by photon counting in time intervals much shorter than the coherence time of the beam under investigation. A long time stability is thus needed and this requirement becomes more and more strict as far as the intensity of light becomes lower. As a matter of fact, most photon counting experiments involved laser beams. Effective photon counters have been also developed, though their current operating conditions are still extreme [4].

The advent of quantum tomography provided a novel method to measure photon distribution [5, 6]. However, the tomography of a state, which have been applied to several quantum states [7], needs the implementation of homodyne detection, which in turn requires the appropriate mode matching of the signal with a suitable local oscillator at a beam splitter.

In this paper, we address a simple method to obtain the photon distribution without directly counting photons. In this scheme, repeated preparations of the signal are revealed through avalanche photodetectors (APD) at different quantum efficiencies. The resulting on/off statistics is then used to reconstruct the photon distribution through maximum-likelihood estimation. Since the model is linear and the photon distribution is a set of positive numbers, then the maximum of the likelihood functional can be found iteratively by the expectation-maximization (EM) algorithm [8, 9]. The method does not require long time stability and involves only simple optical components. The number of experimental runs

depends on the signal under investigation, roughly increasing with its nonclassicality.

The idea of inferring photon distribution through detection at different efficiencies has been already analyzed theoretically [10], and implemented to realize a multichannel fiber loop detector [11]. Here we describe other possible implementations, analyze the reconstruction when only a subset of values $0 < \eta_{\min} < \eta < \eta_{\max} < 1$ of the quantum efficiency is available, and discuss in details the statistical properties of the method: convergence and robustness against fluctuations.

The paper is structured as follows: In Section II we introduce the problem, and show that simple estimation by inversion cannot be used due to lack of precision. Possible implementations of the measurement scheme are also described. Then, in Section III, we illustrate the reconstruction of photon distribution by iterative solution of maximum likelihood estimation. In Section IV the convergence properties of the method, as well as its robustness to fluctuations, are discussed on the basis of several Monte Carlo simulated experiments, performed on different kind of signals. Section V closes the paper with some concluding remarks.

II. ESTIMATION BY INVERSION

Given a single-mode state $\rho = \sum_{n,m} \rho_{nm} |n\rangle\langle m|$ we are interested in the photon distribution, *i.e.* in the set of positive numbers $\rho_n \equiv \rho_{nn} \geq 0$. We assume to have at disposal APDs, which can only discriminate the vacuum from the presence of radiation, with a certain quantum efficiency. This kind of measurement, on/off photodetection, is described by the following probability operator-valued measure (POVM) $\{\Pi_{\text{off}}, \Pi_{\text{on}}\}$

$$\begin{aligned}\Pi_{\text{off}}(\eta) &= \sum_{n=0}^{\infty} (1-\eta)^n |n\rangle\langle n| \\ \Pi_{\text{on}}(\eta) &= \mathbb{I} - \Pi_{\text{off}}\end{aligned}\tag{1}$$

η being the detector's quantum efficiency, *i.e.* the probability that an incoming photon lead to a *click* of the detector. For any given state the detector does not click with a probability $p_{\text{off}}(\eta) = \text{Tr}\{\rho \Pi_{\text{off}}(\eta)\}$, that reads as

^{*}Electronic address: andrea.rossi@mi.infn.it

[†]Electronic address: stefano.olivares@mi.infn.it

[‡]Electronic address: matteo.paris@fisica.unimi.it

follows

$$p_{\text{off}}(\eta) = \sum_{n=0}^{\infty} (1 - \eta)^n \varrho_n. \quad (2)$$

From now on we suppress the subscript “off” and always mean p_{off} when we write p . The “off” probabilities for a set of N detectors measuring the same quantum state with different quantum efficiencies are then

$$\begin{cases} p_0(\eta_0) &= \sum_n (1 - \eta_0)^n \varrho_n \\ p_1(\eta_1) &= \sum_n (1 - \eta_1)^n \varrho_n \\ &\vdots \\ p_N(\eta_N) &= \sum_n (1 - \eta_N)^n \varrho_n \end{cases}. \quad (3)$$

If we know all of the η_ν 's values, equation (3) is a linear system with unknowns $\{\varrho_n\}$. In practice, it is not necessary to have at disposal many detectors with different quantum efficiencies, since a suitable tuning of η can be obtained by optical filters or through an interferometric setup. In fact, besides the fiber loop scheme of [11], different quantum efficiencies can be obtained inserting a set of optical filters before the detector, or by the scheme of Fig. 1 where a single APD is needed, and lower efficiencies are obtained by varying the internal phase-shift ϕ of the interferometer. Since the overall transmissivity of the interferometer is $\tau = \cos^2 \phi$, and a tuning of ϕ of the order of $\pi/500$ can be actually achieved, we may safely assume that about 100 different values of $\eta =$ between $\eta_{\min} \simeq 0$ and $\eta_{\max} = \eta_{\text{APD}}$ can be obtained.

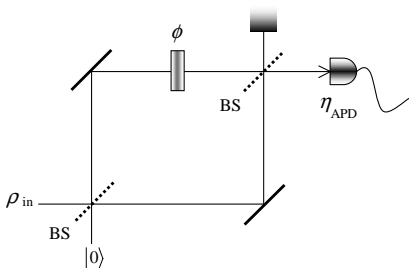


FIG. 1: A possible experimental setup for simulating different quantum efficiencies. The signal passes through an interferometer with internal phase-shift ϕ and is then revealed by a high-efficiency APD. The transmissivity of the interferometer is $\tau = \cos^2 \phi$, and the overall efficiency of photodetection is $\eta = \tau \eta_{\text{APD}}$.

Suppose now that the ϱ_n 's are negligible for $n > \bar{n}$ and that we are able to measure the signal with $N = \bar{n}$ different η 's. In this case equation (3) is a linear system of the form

$$\mathbf{p} = \mathbb{V} \cdot \boldsymbol{\varrho} \quad (4)$$

where

$$\mathbf{p} = \{p_0, p_1, \dots, p_{\bar{n}-1}\}^T \quad (5)$$

$$\boldsymbol{\varrho} = \{\varrho_0, \varrho_1, \dots, \varrho_{\bar{n}-1}\}^T \quad (6)$$

and the coefficients matrix \mathbb{V} (for $\eta_i \neq \eta_j \forall i, j$) is a nonsingular Vandermonde matrix of order \bar{n} . If we put $x_i = 1 - \eta_i$ the \mathbb{V} matrix reads

$$\mathbb{V} = \begin{bmatrix} 1 & x_0 & x_0^2 & \cdots & x_0^{\bar{n}-1} \\ 1 & x_1 & x_1^2 & \cdots & x_1^{\bar{n}-1} \\ \vdots & \vdots & \vdots & \ddots & \vdots \\ 1 & x_{\bar{n}-1} & x_{\bar{n}-1}^2 & \cdots & x_{\bar{n}-1}^{\bar{n}-1} \end{bmatrix}, \quad (7)$$

and the photon distribution can be obtained by matrix inversion $\boldsymbol{\varrho} = \mathbb{V}^{-1} \mathbf{p}$. The same approach can be used also when we are able to reveal the state with $N > \bar{n}$ number of η 's. In this case the system in Eq. (3) should be solved in the least square sense leading to $\boldsymbol{\varrho} = \mathbb{W} \mathbf{p}$, where $\mathbb{W} = (\mathbb{V}^T \mathbb{V})^{-1} \mathbb{V}^T$ is the Moore-Penrose inverse of \mathbb{V} .

Unfortunately, the reconstruction of ϱ_n by matrix inversion cannot be used in practice since it would require an unreasonable number of experimental runs. In fact, most of the quantities x_i entering the expression of \mathbb{V} are of order 10^{-1} , and therefore the \mathbb{V}^{-1} 's entries in the j -th line are of order $x^{-(j-1)}$. This means that the reconstruction of ϱ_j requires the multiplication of the experimental frequencies p_i by quantities of the order $x^{-(j-1)}$, which in turn implies that a sound reconstruction of ϱ_j needs that p_i must be precise at least to the $(j-1)$ -th decimal digit, *i.e.* a minimum of 10^{j-1} experimental runs. In addition, for increasing N and \bar{n} the inversion of (7) must be done numerically leading to errors that quickly become unacceptably large.

III. MAXIMUM-LIKELIHOOD ESTIMATION

The problems illustrated in the previous Section can be circumvented by considering equation (2) as a statistical model for the parameters ϱ_n to be solved by maximum-likelihood (ML) estimation. We assume $N > \bar{n}$ and, for sake of simplicity, we define

$$\begin{aligned} p_\nu &\equiv p_\nu(\eta_\nu), \\ A_{\nu n} &\equiv (1 - \eta_\nu)^n, \end{aligned} \quad (8)$$

so that equations (3) can be rewritten as

$$p_\nu = \sum_n A_{\nu n} \varrho_n. \quad (9)$$

Since the model is linear and the parameters to be estimates are positive (LINPOS problem), then the solution can be obtained using the Expectation-Maximization algorithm (EM) [8, 9]. By imposing the restriction $\sum_n \varrho_n = 1$, we obtain the iterative solution

$$\varrho_n^{(i+1)} = \varrho_n^{(i)} \sum_\nu \frac{A_{\nu n} h_\nu}{C_\nu p_\nu[\{\varrho_n^{(i)}\}]} \quad (10)$$

where $\varrho_n^{(i)}$ is the value of ϱ_n evaluated at i -th iteration, $C_\nu = n_\nu \sum_m A_{\nu m}$, n_ν being the total number of experimental runs with $\eta = \eta_\nu$, h_ν is the number of *no-click*

events for $\eta = \eta_\nu$ and $p_\nu[\{\varrho_n^{(i)}\}]$ are the frequencies p_ν calculated using the reconstructed distribution $\{\varrho_n^{(i)}\}$ at the i -th iteration. By introducing the symbol $f_\nu = h_\nu/n_\nu$ for the experimental frequencies, the expression of $\varrho_n^{(i+1)}$ rewrites as

$$\varrho_n^{(i+1)} = \varrho_n^{(i)} \sum_\nu \frac{A_{\nu n}}{\sum_m A_{\nu m}} \frac{f_\nu}{p_\nu[\{\varrho_n^{(i)}\}]} \dots \quad (11)$$

EM algorithm is known to converge unbiasedly to the ML solution. Indeed, it has been already used to infer the photon distribution from random phase homodyne data [12]. The confidence interval on the determination of the element ϱ_n can be given in terms of the variance $\sigma_n = 1/\sqrt{N F_n}$, N being the number of measurements and F_n the Fisher's information [13]

$$F_n = \sum_\nu \frac{1}{q_\nu} \left(\frac{\partial q_\nu}{\partial \varrho_n} \right)^2, \quad (12)$$

where

$$q_\nu = \frac{p_\nu}{\sum_\nu p_\nu} = \frac{\sum_n A_{\nu n} \varrho_n}{\sum_{\nu n} A_{\nu n} \varrho_n},$$

are the renormalized probabilities of no-click with quantum efficiency η_ν . $N_0 = \sum_{\nu n} A_{\nu n} \varrho_n$ is the global fraction of no-click events (irrespective of the quantum efficiency).

Notice that Eq. (11) provides a solution once an initial distribution $\{\varrho_n^{(0)}\}$ is chosen. In our simulated experiments we start from the uniform distribution $\varrho_n^{(0)} = (1 + \bar{n})^{-1}$ in $[0, \bar{n}]$. Other choices, the only constraint being $\varrho_n^{(0)} \neq 0, \forall n$, do not dramatically influence the convergence properties of the algorithm.

IV. MONTE CARLO SIMULATED EXPERIMENTS AND DISCUSSION

We have performed several numerical simulations in order to check the accuracy and reliability of our method by varying the different parameters. Since our solution of the ML estimation is obtained from an iterative solution, the most important aspect to keep under control is its convergence. As a measure of convergence we use the total absolute error at the k -th iteration

$$\epsilon^{(k)} = \sum_{\nu=0}^N |\epsilon_\nu^{(k)}|, \quad (13)$$

where

$$\epsilon_\nu^{(k)} = p_\nu - p_\nu[\{\varrho_n^{(k)}\}] = p_\nu - \sum_{n=0}^{\bar{n}-1} (1 - \eta_\nu)^n \varrho_n^{(k)}. \quad (14)$$

The total error $\epsilon^{(k)}$ measures the distance of the probabilities $p_\nu[\{\varrho_n^{(k)}\}]$, as calculated at the k -th iteration,

from the actual probabilities as calculated from the theoretical distribution. As a measure of accuracy we adopt the fidelity

$$G^{(k)} = \sum_n \sqrt{\varrho_n \varrho_n^{(k)}} \quad (15)$$

between the reconstructed distribution and the theoretical one. In Figs. 2-4 (right) we report $\epsilon^{(k)}$ versus the number of iterations for different signals. As it is apparent from the plots, the total error is a good marker for the convergence of the algorithm, while the normalization factor $S^{(k)} = \sum_n \varrho_n^{(k)} - 1$ (ideally zero at each step) is not. Notice, however, that the minimum of the total error does not always coincide with the maximum fidelity of reconstruction (Figs. 6 and 7), which means that our method is slightly biased, especially for fast reconstruction, *i.e.* when it converges quickly as it happens for coherent signals. We have numerically observed that this problem can be circumvented by using a number of iterations $n_{it} \simeq n_x$ approximately equal to the number of data. Currently we have no precise explanation of this phenomenon, and provide it as a heuristic prescription leading to best performances for a large class of quantum signals.

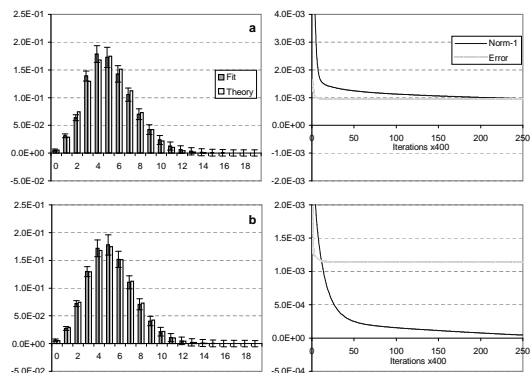


FIG. 2: Reconstruction of the photon distribution of a coherent state $|\alpha\rangle$ with average number of photons $\langle a^\dagger a \rangle \equiv |\alpha|^2 = 5.20$. On the left: the reconstructed photon distribution after $n_{it} = 10^4$ iterations. On the right: the normalization factor $S^{(k)}$ and total error $\epsilon^{(k)}$ (13) as a function of number of iterations. The confidence interval has been evaluated as $1/\sqrt{n_x F_n}$ where F_n is the Fisher information. The number of simulated data and the number of iterations are given by $n_x = n_{it} = 10^5$. In all the simulated experiments $N = 50$ different quantum efficiencies have been used with a minimum efficiency $\eta_{min} = 0.02$. The maximum efficiency is given by: (a) $\eta_{max} = 0.99$; (b) $\eta_{max} = 0.5$. The Hilbert space is truncated at $\bar{n} = 20$.

We have performed simulated experiments for coherent states $|\alpha\rangle = D(\alpha)|0\rangle$, squeezed states $|\alpha, \xi\rangle = D(\alpha)S(\xi)|0\rangle$ and superposition of Fock states $|\psi\rangle = 2^{-1/2}(|n_1\rangle + |n_2\rangle)$, where $D(\alpha) = \exp(\alpha a^\dagger - \bar{\alpha} a)$ is the displacement operator and $S(\xi) = \exp(\frac{1}{2}\xi a^{\dagger 2} - \frac{1}{2}\bar{\xi} a^2)$

is the squeezing operator. Squeezed states have been parametrized through the total average photon number and the squeezing fraction

$$\begin{aligned} \langle a^\dagger a \rangle &= |\alpha|^2 + |\xi|^2 / (1 - |\xi|^2) \\ \zeta &= 1 - |\alpha|^2 / \langle a^\dagger a \rangle. \end{aligned} \quad (16)$$

The value $\zeta = 1$ corresponds to a squeezed vacuum and $\zeta = 0$ to a coherent state. As shown in Fig. 2, the algorithm converges quite fast for coherent states, while for nonclassical states such as squeezed states (Fig. 3) the number of needed iterations is larger. The right plots in Fig. 3 also indicate that increasing N does not always improve accuracy. In Fig. 4 we show reconstruction for the unbalanced superpositions of Fock states $|\psi_2\rangle = (2/3)^{1/2}|2\rangle + (1/3)^{1/2}|7\rangle$.

Concerning the values of the quantum efficiency, we used N values of η uniformly distributed in $[\eta_{\min}, \eta_{\max}]$ with $\eta_{\min} \simeq 0$ and $\eta_{\max} < 1$. In principle, a different distribution (not uniform) may influence the performances of the algorithm. We found, however, that both convergence and accuracy are not much affected by a different choice, which may become relevant only if the spacing between the efficiency values becomes smaller. It should be noticed that the algorithm works well also when η_{\max} is considerably smaller than unit. This is a relevant feature of the method in view of its experimental implementations in different working regimes. In Figs. 2-4 (bottom left) we report the reconstructions obtained assuming $\eta_{\max} = 0.5$ (coherent states and superpositions) and $\eta_{\max} = 0.7$ (squeezed states).

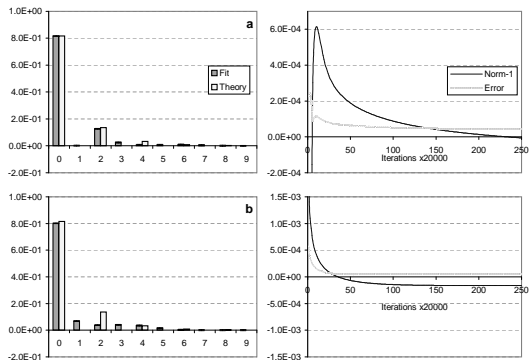


FIG. 3: Reconstruction of the photon distribution of a squeezed state with squeezed fraction $\zeta = 0.99$ and average photon number $\langle a^\dagger a \rangle = 0.5$. Notice that a larger number of iterations is needed in comparison with the coherent signals' case. The number of simulated data and the number of iterations are given by $n_x = 10^5, n_{it} = 5 \times 10^5$. The maximum efficiency is given by: (a) $\eta_{\max} = 0.99$; (b) $\eta_{\max} = 0.7$. The other parameters are the same as in Fig. 2.

In experiments where we have no *a priori* information on the state under investigation it could happen that part, or even most, of the number distribution ϱ_n lies outside the reconstruction region (from 0 to \bar{n}). In this

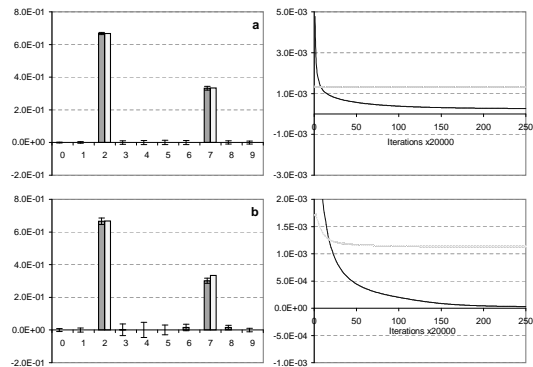


FIG. 4: Reconstruction of the photon distribution of an unbalanced superpositions of number states (see text). The number of simulated data and the number of iterations are given by: (a) $n_x = 10^4, n_{it} = 10^6$; The maximum efficiency is given by: (a) $\eta_{\max} = 0.99$; (b) $\eta_{\max} = 0.5$. The other experimental parameters are the same as in Fig. 2.

case we have checked that the algorithm is able to reconstruct accurately the norm of the included part, such that a simple check of the distribution norm allows to optimize \bar{n} (and in turn N) in few steps. This is a remarkable feature of the algorithm, since in general a large \bar{n} improves convergence but doesn't guarantee better accuracy.

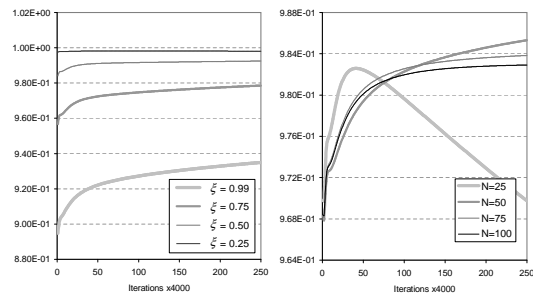


FIG. 5: Fidelity $G^{(k)}$ versus the number of iterations. Left: for a squeezed state with $\langle a^\dagger a \rangle = 1.0$ and different squeezing fractions ζ (left). Right: for a squeezed state with $\langle a^\dagger a \rangle = 1.0$, $\zeta = 0.75$ and different numbers N of η 's values. In both cases the maximum number of iterations is $n_{it} = 10^6$.

The error bars in the plots have been calculated using the Fisher information (12), that explicitly reads:

$$F_n = \frac{1}{N_0^3} \sum_{\nu} \frac{1}{p_{\nu}} \left(A_{\nu n} N_0 - p_{\nu} \sum_k A_{k n} \right)^2, \quad (17)$$

where N_0 is the total number of no click events.

A question may arise about the robustness of the method against fluctuations in the value of the η_{ν} (which, in the case of the interferometric implementation of Fig. 1, may occur as a consequence of *phase* fluctuations), *i.e.* whether or not their precise knowledge is needed.

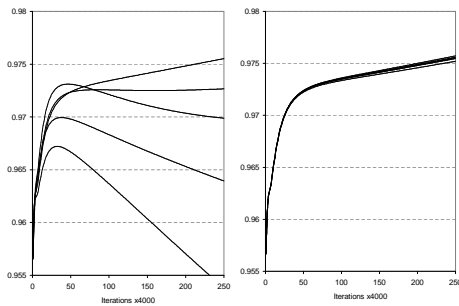


FIG. 6: Fidelity $G^{(k)}$ versus the number of iterations for a squeezed state with $\langle a^\dagger a \rangle = 1.5$ and $\zeta = 0.75$. Each line represent a different simulated run. Left: $n_x = 10^5$, right: $n_x = 10^6$. In both the plot the maximum iterations number is $n_{it} = 10^6$, while the other parameters are the same as in Fig. 2.

In order to check robustness we have performed simulated experiments where, during the run, the quantum efficiency may fluctuate. In particular, we assumed each η_ν uniformly distributed in the range $(-\sigma + \eta_\nu, \sigma + \eta_\nu)$, where

$$\sigma = \frac{\eta_{\max} - \eta_{\min}}{aN}, \quad (18)$$

and a is a positive number. The value $a = 2$ corresponds to each η_ν fluctuating in an interval as large as the spacing $(\eta_{\nu+1} - \eta_\nu)$ around its expected value. The values of p_ν change accordingly during the run. Our results are summarized in Fig. 7. The reconstruction is not dramatically affected by fluctuations, though errors bars are slightly larger. We conclude that the method is robust against fluctuations.

V. CONCLUSIONS

We analyzed in details an iterative algorithm to infer the photon distribution of a single-mode radiation field using only avalanche photodetectors. The method is accurate and statistically reliable for a large class of Gaussian (coherent and squeezed) and non Gaussian states (superpositions and mixtures of $|n\rangle$ states), provided that on/off photodetection may be performed at different quantum efficiencies. The scheme involves only

simple optical components, and allows reconstruction with APD quantum efficiency considerably smaller than unit. The convergence of the method, and its robustness against fluctuations of quantum efficiency have been demonstrated numerically, by means of Monte Carlo simulated experiments.

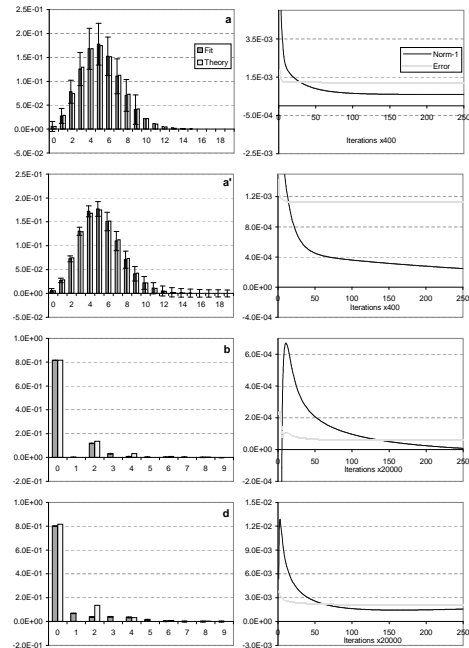


FIG. 7: Reconstruction of the photon distribution for different signals for fluctuating η_ν . (a,a'): coherent state with $\langle a^\dagger a \rangle = 5.20$; (b,b'): squeezed state with $\langle a^\dagger a \rangle = 0.50$ and $\zeta = 0.99$. The number of simulated data and the number of iterations are given by: (a,a') $n_x = 10^5, n_{it} = 10^5$; (b,b') $n_x = 10^6, n_{it} = 5 \times 10^6, \langle a^\dagger a \rangle_{fit} = 5.01$. In all the simulated experiments we set $a = 2$ in Eq. (18). The maximum efficiency is given by: (a,b) $\eta_{\max} = 0.99$; (a') $\eta_{\max} = 0.5$; (b') $\eta_{\max} = 0.7$. The other experimental parameters are the same as in Fig. 2.

Acknowledgments

We thank M. Bondani and A. Ferraro for reading of the manuscript, and Z. Hradil for pointing out relevant references, and for his friendly suggestions. MGAP thanks Marco Genovese for a fruitful discussion.

[1] L. Davidovich, Rev. Mod. Phys. **68**, 127 (1996).
 [2] M. L. Lebedev, A. I. Filin and O. V. Misochnko, Meas. Sci. Technol. **12**, 736 (2001).
 [3] L. Mandel, Rev. Mod. Phys. **71**, S274 (1999).
 [4] J. Kim, S. Takeuchi, Y. Yamamoto, and H.H. Hogue, Appl. Phys. Lett. **74**, 902 (1999); C. Kurtsiefer, S. Mayer, P. Zarda, and H. Weinfurter, Phys. Rev. Lett. **85**, 290

(2000); M. Pelton, C. Santori, J. Vukovic, B. Zhang, G.S. Solomon, J. Plant, and Y. Yamamoto, Phys. Rev. Lett. **89**, 233602 (2002).
 [5] M. Munroe et al., Phys. Rev. A **52**, R924 (1995)
 [6] G. M. D'Ariano, M. G. A. Paris and M. F. Sacchi, Advances in Imaging and Electron Physics **128**, 205 (2003).
 [7] M. Raymer, M. Beck in *Quantum states estimation*, M.

- G .A Paris and J. Řeháček Eds., Lect. Not. Phys. **649** (Springer, Heidelberg, 2004), at press.
- [8] A.P. Dempster, N.M. Laird, D.B. Rubin, J. R. Statist. Soc. B **39**, 1 (1977); Y. Vardi and D. Lee, J. R. Statist. Soc. B **55**, 569 (1993).
- [9] R. A. Boyles, J. R. Statist. Soc. B **45**, 47 (1983); C. F. J. Wu, The Annals of Statistics **11**, 95 (1983).
- [10] D. Mogilevtsev, Opt. Comm **156**, 307 (1998); Acta Phys. Slov. **49**, 743 (1999).
- [11] J. Řeháček, Z. Hradil, O. Haderka, J. Peřina, Jr., and M. Hamar, Phys. Rev. A **67**, 061801(R) (2003); O. Haderka, M. Hamar, J. Peřina, Eur. Phys. Journ. D **28**, (2004).
- [12] K. Banaszek, Acta Phys. Slov. **48**, 185 (1998); Phys. Rev A **57**, 5013 (1998).
- [13] H. Cramer, *Mathematical Methods of Statistics*, Princeton University Press, Princeton, NJ, 1946.